

## Investigating a sequentially assembled MnOx/Pt nanocatalyst as a potential anode for ethylene glycol fuel cells

Ghada H. El-Nowihy<sup>1,\*</sup>, Ahmad M. Mohammad<sup>2</sup>, Mostafa M. H. Khalil<sup>3</sup>, M. A. Sadek<sup>1</sup>,  
Mohamed S. El-Deab<sup>2,\*</sup>

<sup>1</sup> Department of Chemical Engineering, Faculty of Engineering, The British University in Egypt, Cairo, Egypt

<sup>2</sup> Department of Chemistry, Faculty of Science, Cairo University, Cairo, Egypt

<sup>3</sup> Department of Chemistry, Faculty of Science, Ain Shams University, Cairo 11566, Egypt

\*E-mail: [Ghada.Nowihy@bue.edu.eg](mailto:Ghada.Nowihy@bue.edu.eg), [msaada68@yahoo.com](mailto:msaada68@yahoo.com)

Received: 26 September 2016 / Accepted: 6 November 2016 / Published: 12 December 2016

---

Aiming at a better electrocatalytic enhancement of ethylene glycol (EG) electro-oxidation (EGO) in an alkaline medium for EG fuel cells (EGFCs), a MnOx/Pt anode was developed. A sequential layer-by-layer electrodeposition technique was employed to assemble first platinum nanoparticles (nano-Pt) directly onto the surface of a glassy carbon (GC) electrode then manganese oxide nanoparticles (nano-MnOx) were next immobilized. Field emission scanning electron microscopy (FE-SEM) and energy dispersive X-ray spectroscopy (EDS) were employed to evaluate the surface morphology and the bulk composition of the proposed catalyst in addition to the relative ratio of the catalyst's ingredients. On the other hand, the catalyst was characterized electrochemically using cyclic voltammetry (CV) technique. The results manifested the superiority of the developed MnOx/Pt/GC catalyst for enhancing EGO while the degree of enhancement depended on the loading level of the catalyst components and the acidity (pH) of the EG-containing electrolyte. The best electrocatalytic enhancement towards EGO was achieved at MnOx/Pt/GC electrode with nano-Pt = 3.8  $\mu\text{g}$  and nano-MnOx,  $\theta = 52\%$ , in 0.5 M NaOH solution (pH= 11.5) containing 0.5 M EG. Under these conditions, an increase in the oxidation peak current,  $I_p$  (1.7 times) along with a negative shift in the onset potential,  $E_{\text{onset}}$  (ca. 120 mV) of EGO was obtained in reference to the Pt/GC electrode. The developed catalyst exhibited a reasonable catalytic stability upon subjecting for a continuous potential cycling.

---

**Keywords:** Direct ethylene glycol fuel cells; Electrocatalysis; Platinum nanoparticles; Manganese oxide nanoparticles.

## 1. INTRODUCTION

The escalating shortage in energy resources in addition to the indispensable need to green technology have motivated the effort looking for alternative clean and efficient energy resources. These resources are expected to replace the traditional fossil fuel and are supposed to provide high energy density and reduce the polluting emissions without sacrificing the high performance and efficiency.

In this regard, the hydrogen fuel cells (HFCs) generating clean (almost zero emission) electricity from hydrogen appeared efficient, reliable, quiet compact, and environmentally safe [1-5]. That is why the HFCs have been identified as a prime avenue to overcome the world's power shortages. Nevertheless, the HFCs still encounter critical unsafe challenges in the production, use, distribution and storage of the hydrogen gas employed as a fuel. In addition, the energy density produced from the HFCs is relatively low as the electro-oxidation of hydrogen ( $H_2$ ) produces only two electrons. This has propelled the wheel of research towards the liquid fuel cells (LFCs) operated primarily on oxidation of small (low carbon content) organic alcohols (as methanol and propanol) and alcohol-related molecules (formic acid). The boiling point, the hydrogen and carbon contents and the energy density, toxicity are among the key parameters recommending or rejecting a potential liquid fuel from applications in LFCs [6-8].

Compared to direct methanol fuel cells (DMFCs), the direct ethylene glycol (EG) fuel cells (DEGFCs) have a higher volumetric energy density ( $5.90 \text{ kWhL}^{-1}$  vs.  $4.69 \text{ kWhL}^{-1}$ ) and a lower toxicity which make EG an attractive fuel for LFCs [6, 9, 10]. Moreover, the high boiling point of EG permits operation at elevated temperatures with no significant loss (via vaporization) of EG.

Also, DEGFCs is competitive to the direct ethanol fuel cells (DEFCs) in which ethanol is electro-oxidized releasing 12 electrons (in case of complete oxidation into  $CO_2$ ). However, the DEFCs encounter a slow oxidation kinetics (with a rate of electron transfer close to 33%), which consequently lowers the faradaic efficiency of the fuel oxidation [7, 11]. Also, ethanol has a lower ( $78^\circ\text{C}$ ) boiling point than EG preventing the operation at elevated temperatures which is necessary at least for C-C bond cleavage [7, 12]. On the other hand, EG electro-oxidation (EGO) produces 10 electrons (in the case of complete oxidation to  $CO_2$ ) with a higher rate of electron transfer (Ca. 80%) compared to ethanol [7, 13]. In addition, EG has the privilege of possessing a high boiling point ( $198^\circ\text{C}$ ), thus, allowing for operation at elevated temperatures with insignificant loss of EG to the vapor phase, which facilitates the C-C bond cleavage [7, 9, 14-17]. Research is still seeking an improvement for the catalysis of EGO by developing new anodic materials capable to mitigate expected poisoning which may encounter the catalyst during the course of EGO. This research seems essential before going to upscale and commercialize the DEGFCs. Herein we investigate the catalytic activity of a Pt-based electrocatalyst after modification with nano-MnOx towards EGO. It worth mentioning that this catalyst has previously exhibited outstanding catalytic activity towards several electrochemical applications and nano-MnOx has proposed to catalytically mediated these reactions in such a way facilitating the charge transfer and/or removing the poisoning intermediates [10, 18-24]. This investigation also seeks an optimization for the loading level of nano-MnOx onto the Pt/GC surface and the acidity of the EG-containing electrolyte to achieve the best enhancement for EGO.

## 2. EXPERIMENTAL

### 2.1 Abbreviations frequently employed:

The Pt/GC electrode, whenever mentioned, refers to GC electrode after modification with nano-Pt

The MnOx/Pt/GC electrode, as well, refers to proposed catalyst for EGO in which nano-Pt was directly electrodeposited onto the bare GC surface followed by the electrodeposition of nano-MnOx.

### 2.2. Electrodes, pretreatments, and measurements

A GC ( $d = 3.0$  mm) electrode served as the working electrode after polishing mechanically with aqueous slurries of successively finer alumina powder (down to  $0.06$   $\mu\text{m}$ ) and washing with distilled water. An Ag/AgCl/KCl (sat.) and a spiral Pt wire were served as the reference and the counter electrodes, respectively. All potentials in this investigation were referenced to Ag/AgCl/KCl (sat.) electrode. All chemicals were of ultra pure quality (Sigma Aldrich), and did not require to pass by a further purification. Double distilled water was used in the preparation of all aqueous solutions. Electrochemical measurements were performed in aqueous solutions of  $0.5$  M  $\text{H}_2\text{SO}_4$  or  $0.5$  M NaOH in a home-made two-chamber three-electrode glass cell using a Bio-Logic SAS potentiostat (model SP-150) controlled by EC-Lab software. Cyclic voltammograms (CVs) measured in  $0.5$  M  $\text{H}_2\text{SO}_4$  were used to calculate the real surface area of the modified and the unmodified Pt/GC electrodes by calculating the amount of charge associated with the reduction of Pt oxide at ca.  $0.4$  V using a reported value of  $420$   $\mu\text{C cm}^{-2}$  [25]. The calculated surface area was used to determine the surface coverage ( $\theta$ ) of nano-MnOx onto the GC surface. Current densities of EGO CVs were calculated on the basis of the exposed real surface area of Pt at the various electrodes. The effect of pH on the catalytic activity of the proposed catalyst towards EGO was investigated by measuring the electrocatalytic activity in  $\text{H}_2\text{SO}_4$ , NaOH and  $\text{Na}_2\text{SO}_4$  solutions of different pHs of  $0.5$  M EG.

### 2.3. Electrode's modification

The GC electrode modification with nano-Pt was achieved by applying a potential step electrolysis from  $1$  to  $0.1$  V vs. Ag/AgCl/KCl (sat.) for various durations in an aqueous solution of  $0.1$  M  $\text{H}_2\text{SO}_4$  containing  $2.0$  mM  $\text{H}_2[\text{PtCl}_6]$  [10, 18, 19, 26]. A deposition time of  $5$  min (corresponding to  $= 7.5$  mC, ca.  $3.8$   $\mu\text{g}$  Pt) was previously optimized for EGO [27]. Then, the modification of Pt/GC electrode surface with nano-MnOx was performed by cycling the potential between  $0$  and  $0.4$  V vs. Ag/AgCl/KCl (sat.) for several cycles at  $0.02$  V  $\text{s}^{-1}$  in  $0.1$  M  $\text{Na}_2\text{SO}_4$  containing  $0.1$  M  $\text{Mn}(\text{CH}_3\text{COO})_2$  <sup>(10, 18)</sup> resulting in different surface coverage ( $\theta$ ) of nano-MnOx at the nano-Pt surface (*cf* Table 1).

### 2.4. Materials Characterization

A field-emission scanning electron microscope (FE-SEM) (FEI, QUANTA FEG250) coupled with energy dispersive X-ray spectroscopy (EDS-EDAX genitive) was employed to disclose the

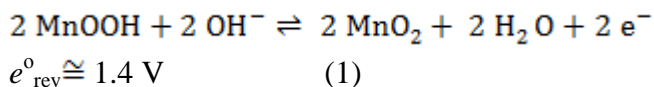
morphology of the various modified GC electrodes and their surface composition, respectively. FE-SEM images were captured at accelerating voltage between 10 and 20 kV with a working distance ranging from 7.8 to 9.9 mm. The top most surface of a cylindrical glassy carbon rod (geometric area = 0.07 cm<sup>2</sup>, 3.0 mm in diameter and 3.0 mm in height) was modified with nano-Pt and nano-MnOx as described above, and then placed in the FE-SEM chamber for surface imaging.

### 3. RESULTS AND DISCUSSION

#### 3.1. Electrochemical and materials characterization

Electrochemical characterization was performed to identify the successful deposition of the electroactive species at the GC electrode surface. Fig. 1 shows CVs measured in (A) acidic (0.5 M H<sub>2</sub>SO<sub>4</sub>) and (B) alkaline (0.5 M NaOH) solutions at (a) Pt/GC and (b) MnOx/Pt/GC electrodes. Obviously, Fig. 1A (curve a), depicts a typical characteristic CV for a clean Pt surface in acidic solutions in which the Pt oxide formation peak extends over a wide range of potential (commences at 620 mV and extends up to 1200 mV). This is coupled with the corresponding Pt oxide reduction peak at ca. 400 mV. In addition, well-defined peaks for H<sub>2</sub> adsorption/desorption (H<sub>ads/des</sub>) appear in the potential range from -300 to 0 mV. The exposed real area of the Pt surface can be calculated from the amount of charge consumed during the Pt oxide reduction peak and/or the H<sub>ads/des</sub> peaks of the Pt. This area of Pt is then used to calculate the surface coverage ( $\theta$ ) of the other catalyst's ingredient (nano-MnOx) which is likely electrodeposited onto the Pt surface (see the caption of Table 1). The intensity of these peaks (Pt oxide reduction and H<sub>ads/des</sub>) decreased as key markers for the further modification of Pt/GC surface with nano-MnOx (Fig. 1A, curve b). The decrease in the intensity of these peaks corresponds to  $\theta$  of nano-MnOx onto Pt/GC surface. Interestingly, an increase in the charging current was observed at 1000-1200 mV at MnOx/Pt/GC electrode (Fig. 1A, curve b) which infers with no confirmation for the deposition of nano-MnOx at Pt/GC surface.

To confirm the successful deposition of nano-MnOx at Pt/GC surface, the same measurements were performed but in an alkaline medium (Fig. 1B). A similar electrochemical behavior to that observed in Fig. 1A (curve a) for a clean Pt surface was observed in Fig. 1B (curve a) but in an alkaline medium. However, another redox couple appeared at ca. -300 mV for MnOx/Pt/GC electrode (Fig. 1B, curve b) and assigned to Mn oxide transformation between lower and higher oxidation states (i.e., MnOOH /MnO<sub>2</sub>) [10, 18-24]:



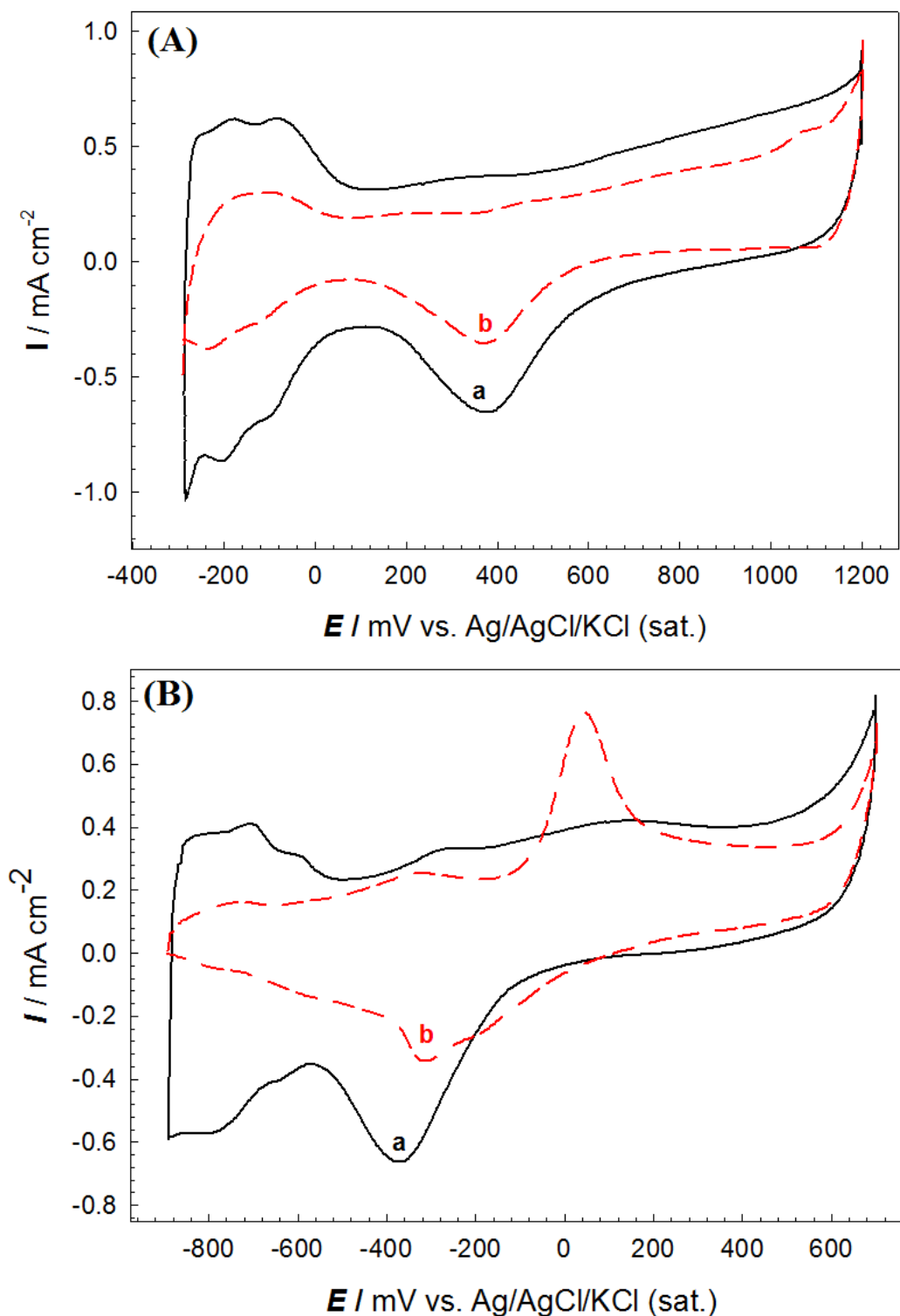


**Figure 1.** CVs measured in (A) deaerated 0.5 M H<sub>2</sub>SO<sub>4</sub> and (B) deaerated 0.5 M NaOH at (a) Pt/GC, (b) MnOx/Pt/GC ( $t_d(\text{Pt}) = 5 \text{ min}$  and  $\theta(\text{MnOx}) = 52\%$ ) electrodes. Potential scan rate =  $0.1 \text{ V s}^{-1}$ . Nano-Pt and nano-MnOx were electrodeposited at the GC surface as described in the experimental section.

The developed MnOx/Pt/GC catalyst was next moved to a morphological characterization using FE-SEM and the relative composition of the catalyst's ingredients were estimated by EDS. Fig.

2A shows the surface view of MnOx/Pt/GC electrode, which indicates the appearance of a network structure of MnOx nanorodes that likely electrodeposited onto the Pt/GC surface. Fig. 2B shows the EDS spectrum of MnOx/Pt/GC electrode, which again confirms the successful deposition of all the catalyst's ingredients and further displays their relative intensities ratio (see the inset of Fig. 2B).

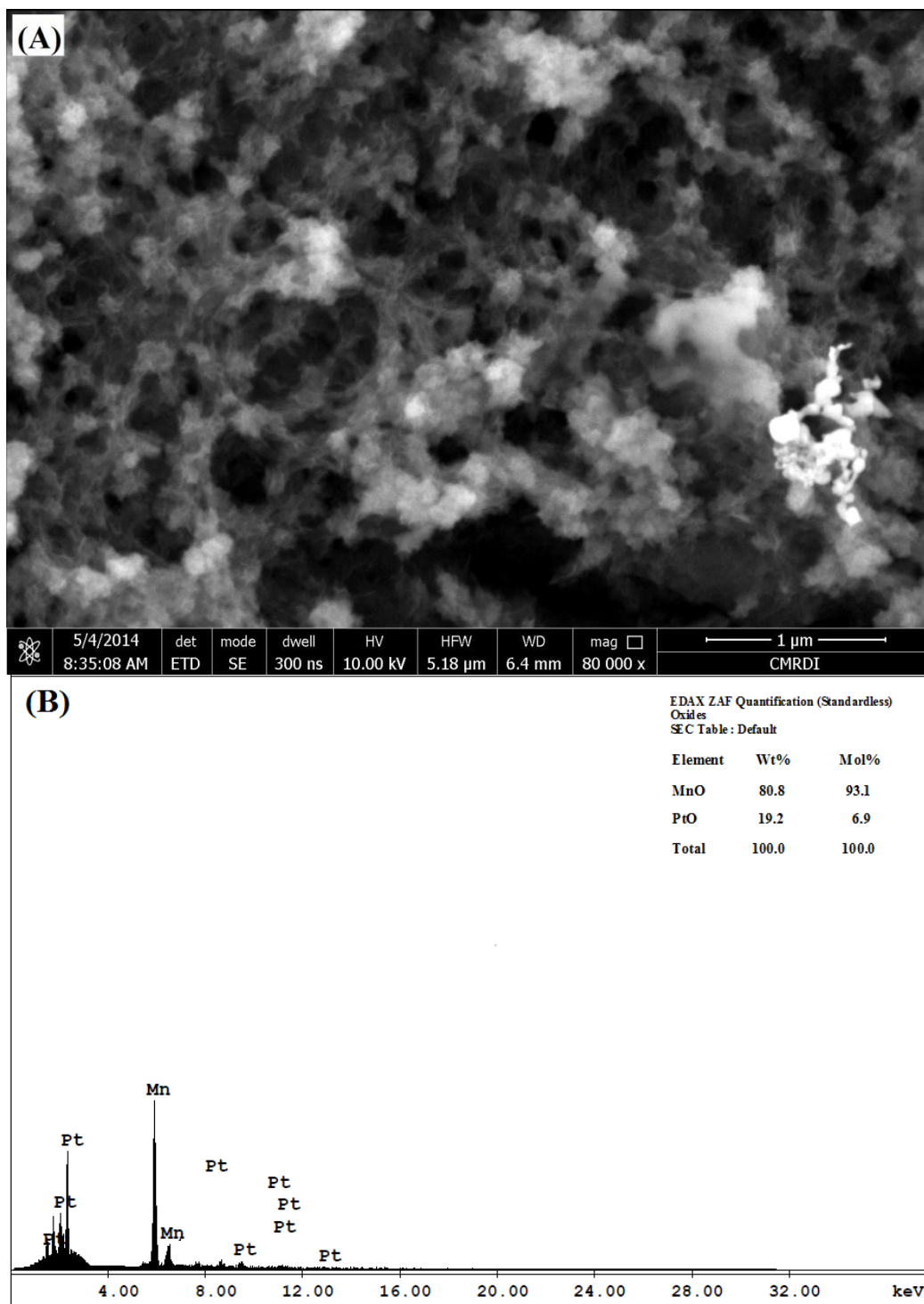


**Figure 2.** (A) FE-SEM image and (B) EDS spectrum of MnOx/Pt/GC electrode. Nano-Pt and nano-MnOx were electrodeposited at the GC surface as mentioned in the caption of Fig. 1.

### 3.2. Optimization of the loading level

The loading level of the catalyst ingredients (i.e., nano-Pt and nano-MnOx) in the proposed catalyst (MnOx/Pt/GC) is expected to influence the catalytic activity towards EGO. In a previous work, we have optimized the loading level of nano-Pt at the GC surface towards EGO [27]. A deposition time for nano-Pt ( $t_{d(Pt)}$ ) of 5 min resulted in the deposition of 3.8  $\mu\text{g}$  of nano-Pt and that was optimum for EGO on the Pt/GC electrode.

Even with utilizing the optimum loading of nano-Pt the catalytic enhancement for EGO is not the desired value encouraging for a fast commercialization. Hence, another promising ingredient (nano-MnOx) was added to the catalyst composition. We believe that transition metal oxides as nano-MnOx are able to catalytically mediate EGO via MnOOH/MnO<sub>2</sub> transformation in such a way facilitating the charge transfer and/or getting rid the poisoning intermediates during several steps of EGO via [10, 18-24]:

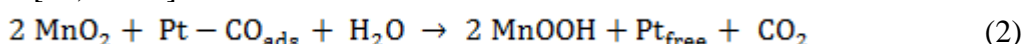
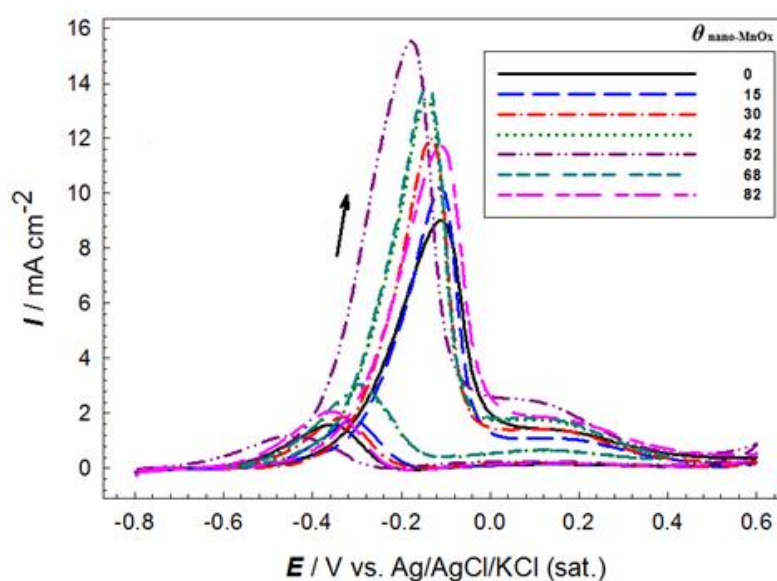


Fig. 3 shows the impact of nano-MnOx loading level on the catalytic activity towards EGO. That is an increase in  $I_p$  together with a negative shift in  $E_{\text{onset}}$  of EGO were initially observed with the increase in  $\theta$  which continued increasing up to  $\theta = 52\%$  (equivalent to nano-MnOx electrodeposited by 40 deposition cycles). At this coverage, the highest  $I_p$  (ca. 1.7 times) and the largest negative shift of  $E_{\text{onset}}$  (ca. 120 mV) of EGO were obtained at the MnOx/Pt/GC in comparison to the Pt/GC electrode. Increasing the deposition cycles of nano-MnOx, beyond 40 cycles (i.e.,  $\theta = 52\%$ ) reduces the catalytic activity (see Fig. 3 and Table 1). A plausible explanation for this observation is that the excessive deposition of nano-MnOx consumed more active sites of nano-Pt which was proved previously to be essential EGO [27].



**Figure 3.** CVs for EGO at MnOx/Pt/GC (different deposition cycles of nano-MnOx while maintaining the same  $t_{d(Pt)} = 5$  min) electrodes in 0.5 M NaOH solutions containing 0.5 M EG. Potential scan rate is 0.05 V s<sup>-1</sup>.

**Table 1.** Variation of the catalytic enhancement factor and the onset potential for EGO with different deposition cycles of nano-MnOx onto Pt/GC (nano-Pt loading was kept constant at 3.8  $\mu\text{g}$ ) in 0.5 M NaOH + 0.5 M EG.

No. of deposition cycles of nano-MnOx	Surface coverage <sup>a</sup> / $\theta$ ,%	$E_{\text{onset}}$ <sup>b</sup> /mV	$I_p$ /mA cm <sup>-2</sup>	Enhancement factor <sup>c</sup>
0	-----	-460	9.0	-----
10	15	-480	10.2	1.13
20	30	-500	12.0	1.33
30	42	-520	13.4	1.48
40	52	-580	15.5	1.72
50	68	-540	13.9	1.54
60	82	-460	11.5	1.27

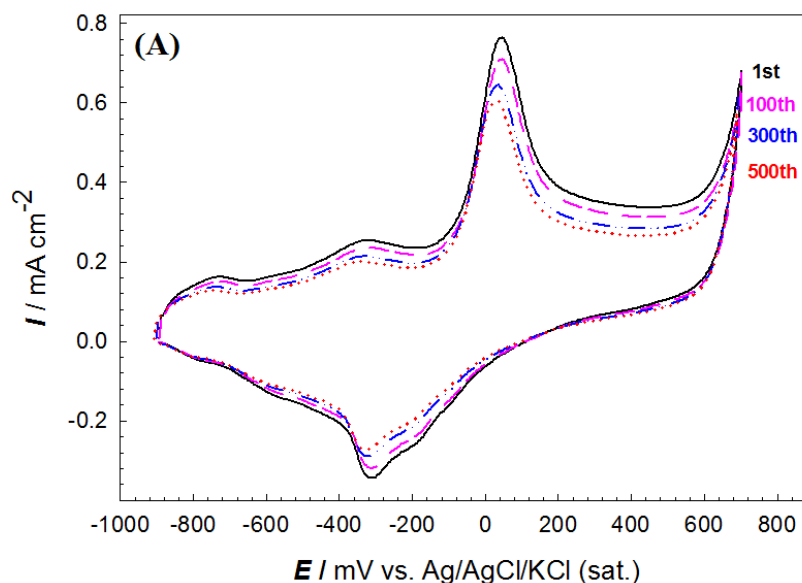
<sup>a</sup> The values of surface coverage ( $\theta$ ) were calculated for the various modified Pt/GC electrodes where ( $\theta = 1 - S_{\text{modified}}/S_{\text{unmodified}}$ ).  $S_{\text{modified}}$  and  $S_{\text{unmodified}}$  refer to the real surface area of the modified and the unmodified Pt/GC electrodes, respectively, obtained from the amount of charge associated with the reduction of Pt oxide at ca. 0.4 V (Fig. 1A) using a reported value of 420  $\mu\text{C cm}^{-2}$  [25].

<sup>b</sup> Estimated at a constant current density of 100  $\mu\text{A cm}^{-2}$  for all electrodes.

<sup>c</sup> The enhancement factor for EGO is calculated by dividing  $I_p$  of EGO obtained at the metal oxide-modified Pt/GC electrodes by  $I_p$  of EGO at Pt/GC electrode.

### 3.3. Effect of aging

The stability of MnOx/Pt/GC electrode has been studied by examining the effect of ageing of such electrode ( $t_d(\text{Pt}) = 5$  min and MnOx,  $\theta = 52\%$ ) towards the electrocatalytic activity of EGO. It is performed by cycling the potential several times at MnOx/Pt/GC electrode in alkaline medium (0.5 M NaOH) and recording the corresponding CVs response towards EGO.



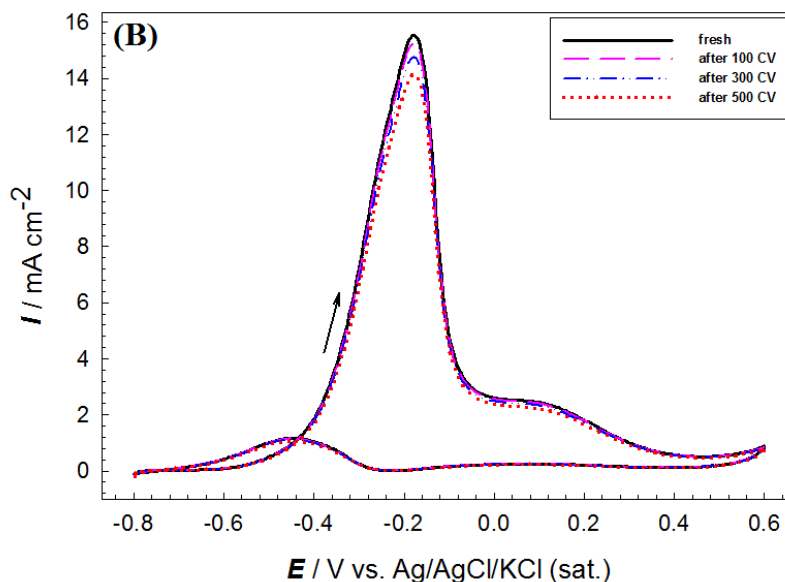


**Figure 4.** (A) CVs responses at MnOx/Pt/GC electrode in 0.5 M NaOH after ageing for several potential cycles (1st, 100, 300 and 500 potential cycles). (B) CVs for EGO at MnOx/Pt/GC electrode ( $t_{d(Pt)} = 5$  min and MnOx,  $\theta = 52\%$ ) in 0.5 M NaOH solutions containing 0.5 M EG after aging for several potential cycles (1st, 100, 300 and 500 potential cycles). Potential scan rate is  $0.05 \text{ V s}^{-1}$ .

Fig. 4A shows the CVs of MnOx/Pt/GC electrode in 0.5 M NaOH after ageing for 100, 300, and 500 potential scans. Interestingly, a stable redox behavior for MnOOH/MnO<sub>2</sub> with almost a minor decrease in the peak currents was obtained, indicating the high stability of MnOx/Pt/GC electrode in the current operating pH and conditions. The corresponding CVs of EGO at the same electrode in 0.5 M NaOH solution containing 0.5 M EG are shown in Fig. 4B. Interestingly, the  $E_{\text{onset}}$  of EGO remained the same but  $I_p$  of EGO decreased slightly indicating a slower kinetics of EGO with the number of aging cycles. Hence, we can safely say that the developed catalyst (MnOx/Pt/GC) is stable over prolonged time of electrolysis.

Interestingly, the catalytic activity towards EGO obtained in this investigation at MnOx/Pt/GC ( $t_{d(Pt)} = 5$  min and MnOx,  $\theta = 52\%$ ) catalyst was superior if compared to earlier results reported using Pt–Ru/CNT and Pt/CNT catalysts. That appeared in the large increase in  $I_p$  ( $15.5 \text{ mA cm}^{-2}$ ) for EGO at MnOx/Pt/GC if compared to 13 and  $7 \text{ mA cm}^{-2}$ , which were, respectively, obtained at Pt–Ru/CNT and Pt/CNT catalysts [28]. The current decay of EGO after 500 cycles of continuous electrolysis was as well minimum (9.7%) at MnOx/Pt/GC catalyst but was much higher (19.2 and 42.9 %) employing the Pt–Ru/CNT and Pt/CNT catalysts, respectively [28]. These indicates precisely the excellence of the developed catalyst (MnOx/Pt/GC electrode) for EGO.

### 3.4. Effect of pH

Fig. 5 shows the influence of the pH of the EG-containing electrolyte on the electrocatalytic activity of MnOx/Pt/GC electrode towards EGO. It reveals that EGO is a pH dependent reaction. The peak current ( $I_p$ ) of EGO increases with pH (see Table 2). It is believed that, in acidic media, nano-

MnOx electrocatalyst is neither chemically nor mechanically stable, leading to a significant lowering in the observed catalytic activity [29-32]. On the other hand, the enhanced activity of EGO in alkaline medium is related to the relative stability of nano-MnOx together with the facilitated oxidation of poisoning intermediates (e.g., CO-like intermediates) by  $\text{OH}^-$  ions (source of oxygen providing species) according to Langmuir–Hinshelwood mechanism [33-35].

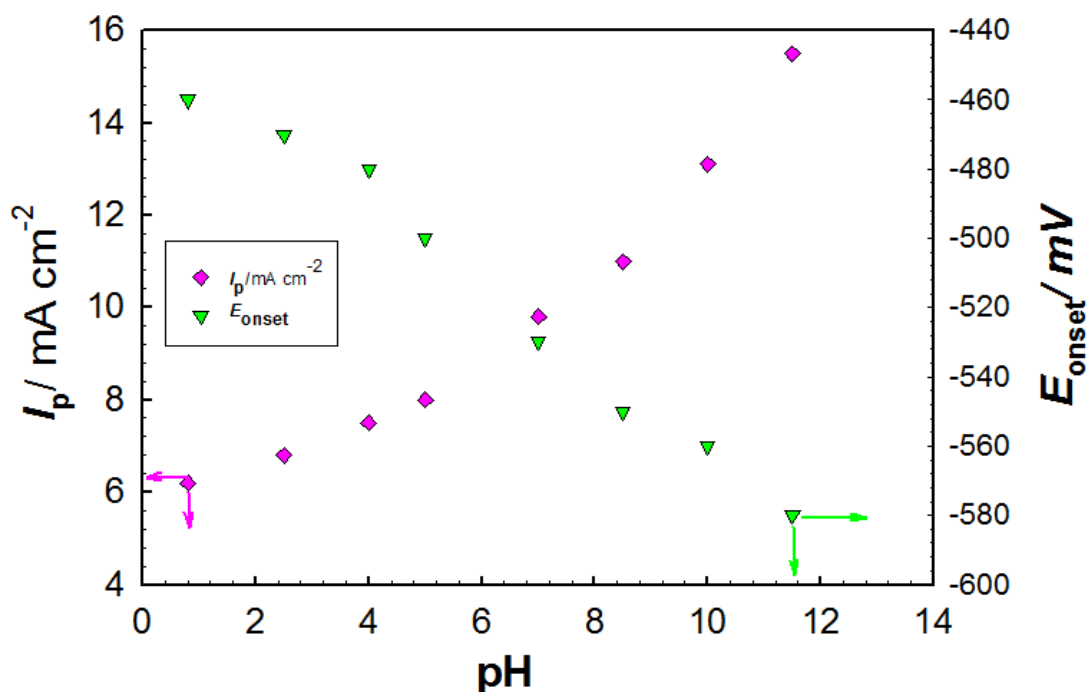
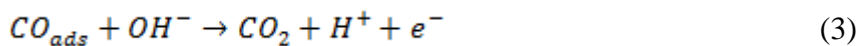


**Figure 5.** Variation of oxidation peak current ( $I_p$ ) and onset potential ( $E_{\text{onset}}$ ) of EGO with pH obtained at MnOx/Pt/GC electrode ( $t_d(\text{Pt}) = 5$  min and MnOx,  $\theta = 52\%$ ).

**Table 2.** Variation of oxidation peak current ( $I_p$ ) of EGO obtained at MnOx/Pt/GC electrode in aqueous solution of 0.5 M EG with various pH values (Note that the solution pH is adjusted by the addition of proper amounts of  $\text{Na}_2\text{SO}_4$  and/or  $\text{H}_2\text{SO}_4$ ).

pH	$I_p / \text{mA cm}^{-2}$	$E_{\text{onset}} / \text{mV}$
0.8	6.2	-460
2.5	6.8	-470
4.0	7.5	-480
5.0	8.0	-500
7.0	9.8	-530
8.5	11.0	-550
10.0	13.1	-560
11.5	15.5	-580

#### 4. CONCLUSION

An electrochemically modified GC electrode by a binary catalyst composed of nano-Pt and nano-MnOx was proposed for the efficient electrocatalytic enhancement of ethylene glycol oxidation (EGO). The influence of the loading level of the catalyst ingredients on the catalytic activity towards EGO followed a volcano trend. At MnOx/Pt/GC electrode, with nano-Pt loading = 3.8  $\mu\text{g}$  and nano-MnOx surface coverage ( $\theta$ ) = 52%, the highest catalytic enhancement for EGO was achieved. The enhancement in the catalytic activity is most likely originated from a catalytic mediation by nano-MnOx during EGO in such a way facilitating the charge transfer and/or removing the poisoning intermediates. As well, this electrode showed a reasonable stability after aging for several potential cycles. Moreover, EGO found to be pH dependent.

#### References

1. D.-H. Lee and C.-P. Hung, *Int. J. Hydrogen Energy*, 37 (2012) 15753.
2. H. L. Hellman and R. van den Hoed, *Int. J. Hydrogen Energy*, 32 (2007) 305.
3. A. Kirubakaran, S. Jain, and R.K. Nema, *Renewable and Sustainable Energy Reviews*, 13 (2009) 2430.
4. J. M. Feliu and E. Herrero, *Handbook of Fuel Cells*, ed. W. Vielstich, H.A. Gasteiger, and A. Lamm. 2 (2003), New York: Wiley.
5. A. M. Abdullah, A. M. Mohammad, T. Okajima, F. Kitamura and T. Ohsaka, *J. Power Sources*, 190 (2009) 264.
6. E. Antolini and E.R. Gonzalez, *J. Power Sources*, 195 (2010) 3431.
7. L. An, L. Zeng, and T.S. Zhao, *Int. J. Hydrogen Energy*, 38 (2013) 10602.
8. L. Demarconnay, S. Brimaud, C. Coutanceau and J.-M. Leger, *J. Electroanal. Chem.*, 601 (2007) 169.
9. L. Xin, Z. Zhang, J. Qi, D. Chadderdon and W. Li, *Appl. Catalysis B*, 125 (2012) 85.
10. A. M. Mohammad, G. H. El-Nowihy, M. M. H. Khalil and M. S. El-Deab, *J. Electrochem. Soc.*, 161 (2014) F1340.
11. L. An, T.S. Zhao, and J.B. Xu, *Int. J. Hydrogen Energy*, 36 (2011) 13089.
12. C. Bianchini, V. Bamburgioni, J. Filippi, A. Marchionni, F. Vizza, P. Bert and A. Tampucci, *Electrochem. Commun.*, 11 (2009) 1077.
13. L. An, T. S. Zhao, S. Y. Shen, Q. X. Wu and R. Chen, *Int. J. Hydrogen Energy*, 35 (2010) 4329.
14. C. Cremersa, A. Niedergesäß, F. Junga, D. Müllera and J. Tübkea, *ECS Trans*, 41 (2011) 1987.
15. K. Matsuoka, Y. Iriyama, T. Abe, M. Matsuoka and Z. Ogumi, *J. Power Sources*, 150 (2005) 27.
16. Z. r. r. Ogumi, K. Matsuoka, S. Chiba, M. Matsuoka, Y. Iriyama, T. k. r. r. Abe and M. Inaba, *Electrochemistry*, 70 (2002) 980.
17. K. Miyazaki, T. Matsumiya, T. Abe, H. Kurata, T. Fukutsuka, K. Kojima and Z. Ogumi, *Electrochim. Acta*, 56 (2011) 7610.
18. G. H. El-Nowihy, A. M. Mohammad, M. M. H. Khalil and M. S. El-Deab, *Int. J. Electrochem. Sci.*, 9 (2014) 5177.
19. M. S. El-Deab, G.H. El-Nowihy, and A.M. Mohammad, *Electrochim. Acta*, 165 (2015) 402.
20. M. S. El-Deab, *Int. J. Electrochem. Sci.*, 4 (2009) 1329.
21. S. Ardizzone, and S. Trasatti, *Adv. Colloid and Interface Sci.*, 64 (1996) 173.
22. El-Deab, M.S. and T. Ohsaka, *J. Electrochem. Soc.*, 155 (2008) D14.

23. S. p. Fierro, T. Nagel, H. Baltruschat and C. Comninellis, *Electrochem. Commun.*, 9 (2007) 1969.
24. M. Pourbaix, *Atlas of Electrochemical Equilibria in Aqueous Solutions*. (1966) 286, Pergamon Press: Oxford.
25. S. Trasatti and O. A. Petrii, *Pure & Appl. Chem.*, 63 (1991) 711.
26. M. S. El-Deab, *J. Adv. Res.*, 3 (2012) 65.
27. Ghada H. El-Nowihy, Ahmad M. Mohammad, Mostafa M. H. Khalil, M. A. Sadek and M. S. El-Deab, *submitted to Int. J. Hydrogen Energy* (2016).
28. V. Selvaraj, M. Vinoba and M. Alagar, *J. Colloid Interface Sci.*, 322 (2008) 537
29. M. Pourbaix, *Atlas of Electrochemical Equilibria in Aqueous Solutions*. 2nd ed. (1974), Texas: NACE. Houston.
30. I. M. Sadiq, A. M. Mohammad, M. E. El-Shakre, M. I. Awad, M. S. El-Deab and B. E. El-Anadouli, *Int. J. Electrochem. Sci.*, 7 (2012) 3350.
31. R. C. Hubli, J. Mittra, and A.K. Suri, *Hydrometallurgy*, 44 (1997) 125.
32. E. A. Yakusheva, I. G. Gorichev, T. K. Atanasyan and Y. A. Lainer, *Russ. Metall.*, 2010 (2010) 18.
33. H. Kita, K. Shimazu, and K. Kunimatsu, *J. Electroanal. Chem., Interfacial Electrochem.*, 241 (1988) 163.
34. J. S. Spendelow, J. D. Goodpaster, P. J. A. Kenis and A. Wieckowski, *J. Phys. Chem. B*, 110 (2006) 9545.
35. K. D. Popovic, J. D. Lovic, A.V. Tripkovic and P. K. Olszewski, *J. Serb. Chem. Soc.*, 74 (2009) 965.

© 2017 The Authors. Published by ESG ([www.electrochemsci.org](http://www.electrochemsci.org)). This article is an open access article distributed under the terms and conditions of the Creative Commons Attribution license (<http://creativecommons.org/licenses/by/4.0/>).